Journal of Integrative Neuroscience

J. Integr. Neurosci. **2025**; 24(12): 46980
https://doi.org/10.31083/JIN46980

Original Research

Acupuncture Modulates NMDAR-PP1/Calpain1-KCC2 Pathway to Ameliorate Spinal Hyperexcitability and Spastic Hemiplegia Induced by Ischemic Stroke

Jia-Ling He[1], Liang-Xiao Ma[1,2,*], Yu-Xin Zhuang[1], Jing-Si Wen[1], Ling-Hui Ma[1], Jing-Yun Xiu[1], Meng-Yu Chen[1]

[1]School of Acupuncture-Moxibustion and Tuina, Beijing University of Chinese Medicine, 100029 Beijing, China
[2]The Key Unit of State Administration of Traditional Chinese Medicine, Evaluation of Characteristic Acupuncture Therapy, 100029 Beijing, China
*Correspondence: maliangxiao@vip.sina.com (Liang-Xiao Ma)

Academic Editor: Moo-Ho Won
Submitted: 28 September 2025 Revised: 7 November 2025 Accepted: 19 November 2025 Published: 26 December 2025

Abstract

Background: Post-stroke spastic hemiplegia (PSSH) frequently leads to severe motor dysfunction, with its primary pathology being spinal hyperexcitability arising from attenuated descending inhibition. We previously reported that acupuncture alleviated spastic hypertonia induced by middle cerebral artery occlusion (MCAO) via upregulating potassium-chloride cotransporter 2 (KCC2) expression. Cumulative evidence has indicated that N-methyl-D-aspartate receptor (NMDAR) can be a pivotal determinant of spinal excitability via modulating KCC2-mediated neuronal chloride homeostasis. The present study investigated whether acupuncture exerts its therapeutic effects through modulation of NMDAR-mediated activation of protein phosphatase 1 (PP1)/Calpain1-KCC2 pathway. **Methods**: Multiple functional assessments, *in vivo* electrophysiological test, 2,3,5-triphenyl tetrazolium chloride (TTC) staining, immunofluorescence, quantitative real-time PCR (RT-qPCR), and Western blot were used. **Results**: In the male MCAO rat model, assessments using the neurological-function score, muscle-tone scale, and footprint analysis demonstrated that acupuncture significantly attenuated spasticity and improved motor performance. H-reflex recordings and immediate early gene c-Fos (c-Fos) immunofluorescence indicated that acupuncture reduced hyperexcitability in spinal ventral horn. These observed effects of acupuncture were associated with its downregulation of N-methyl-D-aspartate receptor 1 (NMDAR1) expression and restoration of both the expression and function of KCC2 in spinal cord. Pharmacological interventions using NMDAR agonist and antagonist demonstrated that acupuncture upregulated KCC2 by inhibiting NMDAR-mediated activation of PP1 and Calpain1. **Conclusion**: Acupuncture modulated the NMDAR-PP1/Calpain1-KCC2 pathway in the spinal cord to suppress neuronal hyperexcitability, thereby relieving spasticity and promoting motor function in rats with PSSH.

Keywords: stroke; spastic hemiplegia; NMDA receptor; KCC2 cotransporter; acupuncture

1. Introduction

As a highly prevalent complication in stroke survivors, post-stroke spastic hemiplegia (PSSH) is distinguished by increased muscle tone and abnormal movement patterns dominated by spasticity, which has a profound effect on patients' quality of life and places a considerable strain on healthcare systems [1–3]. After stroke, the obstruction of cerebral blood vessels leads to ischemic damage in the affected brain tissue, causing an impaired transmission of voluntary motor commands and inhibitory signals. It leads to hyperexcitability in the spinal ventral horn, causing involuntary muscle contractions and spastic hypertonia, which ultimately presents as spastic hemiplegia [4,5]. Neuronal-excitability regulation is a complex process that involves the coordinated action of various neurotransmitters, receptors, and intracellular signaling pathways.

N-methyl-D-aspartate receptor (NMDAR) is an ionotropic glutamate receptor widely distributed on the motor neurons in spinal ventral horn. It has high Ca^{2+} permeability and slow activation and deactivation kinetics [6]. This enables NMDAR to serve as a key determinant in regulating neuronal excitability and mediating excitotoxicity [7,8]. Potassium-chloride cotransporter 2 (KCC2) is a key transport protein located on the neuronal membrane. It extrudes intracellular Cl^-, thereby maintaining a low intracellular Cl^- concentration and providing the necessary conditions for γ-aminobutyric acid (GABA) A-type receptor mediated Cl^- influx and subsequent membrane hyperpolarization. This allows it to effectively inhibit excessive excitability of neurons [9,10]. Emerging evidence has suggested that pathological NMDAR overactivation may impair KCC2 function through multiple downstream pathways, including protein phosphatase 1 (PP1)-mediated dephosphorylation and calpain1-dependent proteolytic degradation [11,12]. These mechanisms converge to disrupt GABAergic inhibition and exacerbate neuronal hyperexcitability.

Commonly used drugs, such as baclofen, alleviate increased muscle tone by activating $GABA_B$ receptors to inhibit neuronal excitability [13]. Nevertheless, these drugs often show limited efficacy, with short-term effects and potential side effects. Acupuncture, as a non-pharmacological therapeutic approach, has garnered widespread attention in recent years for its enduring efficacy, simplicity, and cost-effectiveness in treating PSSH [14–16]. Previous research has observed that, in rat models of spinal cord injury resulting in motor dysfunction, NMDAR in the spinal cord was elevated, and is effectively reversed by electroacupuncture [17]. Additionally, in rats with middle cerebral artery occlusion (MCAO) exhibiting hypertonia, the expression levels of KCC2 and $GABA_A$ in the spinal cord were reduced; acupuncture restored their expression, alleviated spasticity, and promoted motor-function recovery [18]. However, how acupuncture modulates neuronal excitability through the coordinated action of NMDAR and KCC2 remains insufficiently understood. The present study investigated whether acupuncture exerts its therapeutic effects on PSSH through the regulation of the NMDAR-PP1/Calpain1-KCC2 pathway.

2. Materials and Methods

2.1 Animals

Male Sprague-Dawley rats (8 weeks), ranging in weight from 250 to 280 g, were used for the study. All rats were kept in cages of 4 under SPF conditions at room temperature (23 $\pm$ 2 °C) under a 12:12 h light/dark cycle. The rats had unrestricted access to standard laboratory chow and tap water.

2.2 Experimental Design

The experimental timeline and corresponding procedures are shown in Fig. 1A and Fig. 5A. To evaluate the effects of acupuncture on rats with PSSH, four groups were established: Sham-operated group (Sham), MCAO induced PSSH model group (Model), acupuncture at acupoint group (Acup), and acupuncture at control point (non-acupoint) group (CP). To investigate the role of NMDAR, the NMDAR agonist NMDA and antagonist D-(-)-2-Amino-5-phosphonopentanoic acid (D-AP5) were administered. Five groups were established: Model, Model + vehicle, Acup + vehicle, Model + D-AP5, and Acup + NMDA. All rats were randomly assigned to these groups. Excluding the 10 rats that underwent sham surgery, 112 rats were subjected to MCAO procedure for PSSH-model induction, of which 80 were successfully modeled and subsequently used in the experiments (**Supplementary Table 1**). The sample size was chosen according to previous research and our preliminary data, ensuring adequate statistical power to identify meaningful differences among groups.

2.3 MCAO Surgery

The permanent MCAO procedure was performed to establish a PSSH model, following the previously described method with slight modifications [19,20]. After anesthetization with isoflurane (3% in oxygen; flow rate, 1 L/min; cat. no. R510-22-10; RWD Life Science, Shenzhen, Guangdong, China), a midline skin incision was performed on the ventral neck to expose the right common carotid artery. A silicone-coated nylon monofilament with a diameter of 0.36 mm (Beijing Cinontech Co., Ltd.; Beijing, China) was gently advanced from the right external carotid artery to the internal carotid artery and further to the origin of the middle cerebral artery (MCA). The filament was left in place for the remainder of the experiment. A temperature-controlled heated pad was applied during the ischemic period to maintain the body temperature constantly at 37 $\pm$ 0.5 °C. In sham-operated rats, the identical surgical procedure was carried out but without occlusion of the MCA.

MCAO rats were included in the study if they exhibited a regional cerebral blood flow (CBF) reduction of greater than 70% of baseline levels, and a Zea-Longa score above 1. All behavioral evaluations were performed by an independent investigator who was blind to the interventions of the study.

2.4 Laser Speckle Imaging

CBF changes were assessed using a laser speckle imaging system (PeriCam PSI NR; Perimed AB; Stockholm, Sweden). Measurements were taken 5 min before and 5 min after MCAO surgery to determine relative perfusion in the MCA territory. After induction of anesthesia, a midline scalp incision was made to expose the skull. Circular regions of interest (ROIs) with a diameter of 2 mm were placed 3 mm lateral and 2 mm posterior to the bregma on the right cortical surface (Fig. 1B). CBF values were calculated as percentages relative to pre-occlusion baseline levels according to acquired microcirculation images.

2.5 Acupuncture and Drug Treatment

Acupuncture treatment was administered once daily to rats in the Acup and CP groups from postoperative day 4 to day 10. Sterile, disposable acupuncture needles (0.25 $\times$ 13 mm; Zhongyantaihe; Tianjin, China) were perpendicularly inserted into the "Yanglingquan" (GB34) acupoint, located in the depression distal to the head of the fibula on the left hind limb (Fig. 1C). The needle was inserted 4–5 mm deep and manipulated with multi-directional lifting and thrusting combined with passive movement of affected hind limb, then retained in place for 30 min. In the CP group, needles were superficially inserted into a non-acupoint at the midpoint of the tail, a site not corresponding to any recognized acupuncture-point location.

NMDA (40 mM, cat. no. 0114; Tocris; Minneapolis, MN, USA) and D-AP5 (15 mM, cat. no. 0106; Tocris)

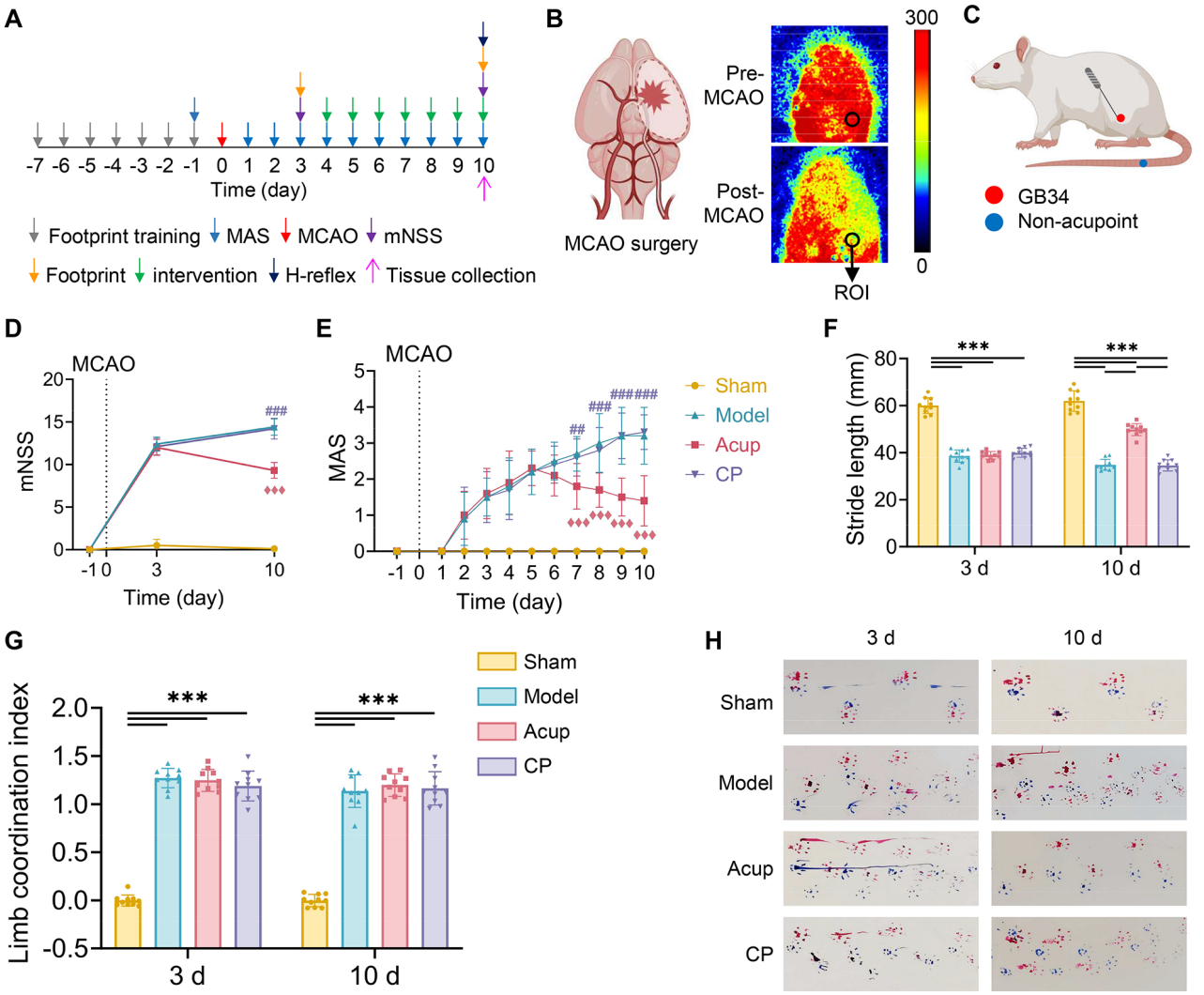

Fig. 1. Acupuncture alleviates spasticity and enhances motor function in MCAO rats with PSSH. (A) Timeline of experimental procedures. (B) Representative laser speckle images (LSI) for monitoring cortical blood flow (CBF) after MCAO surgery. (C) Acupuncture site location. (D) Neurological deficits assessed by the mNSS. (E) Muscle tone assessed by the MAS. (F) Stride length of rats at 3 days and 10 days. (G) Limb coordination index of rats at 3 days and 10 days. (H) Footprints of rats in each group, with blue representing the forelimbs and red representing the hind limbs. N = 10 per group. Data are presented as mean ± SD. $^{♦♦♦}p < 0.001$ compared to the Model group; $^{\#\#}p < 0.01$, $^{\#\#\#}p < 0.001$ compared to the Acup group; $^{***}p < 0.001$. MAS, modified ashworth scale; MCAO, middle cerebral artery occlusion; mNSS, modified neurological severity score; GB34, Yanglingquan; d, day; PSSH, post-stroke spastic hemiplegia. Sham: Sham-operated group; Model: MCAO induced PSSH model group; Acup: acupuncture at acupoint group; CP: acupuncture at control point (non-acupoint) group. Fig. 1B and Fig. 1C Created with BioRender.com.

were used for NMDAR modulation. Both compounds were freshly dissolved in sterile distilled water and administered via intrathecal injection at a volume of 30 µL once daily from postoperative day 4 to day 10.

2.6 Neurobehavioral Tests

2.6.1 Neurological Deficit Assessment

The modified Neurological Severity Score (mNSS) was used to assess overall neurological function, including motor ability, sensory responses, reflexes, and balance [21]. In this scoring system, one point is assigned for the inability to perform a task or for the absence of a reflex. Neurological function was scored on a scale from 0 to 18, where 0 indicated normal function and 18 represented the maximum deficit.

2.6.2 Muscle Tone Assessment

The Modified Ashworth Scale (MAS) was used to assess muscle tone in the affected hind limb [22]. The scale ranges from 0 to 4 (normal muscle tone with free limb movement, 0; complete rigidity of limbs, 4) [18]. A higher

score indicates higher muscle tone and greater limitation of joint movements. In this study, the maximum MAS score was set to 5, with scores of 1+ converted to 2 for analysis purposes [23].

2.6.3 Footprint Analysis

Walking-track-footprint analysis was described previously [24]. Rats had their forepaws dipped in nontoxic blue dye and hind paws in red dye. Each rat was placed at the start of an 80-cm-long, 10-cm-wide wooden track leading to a darkened goal box containing food. Prior to surgery, each rat underwent one training session per day to ensure consistent gait. During each testing session, the rat traversed the track, leaving footprints on white paper. Trials were repeated if the rat hesitated, stopped, or failed to complete the walk smoothly. For each rat, 6 consecutive hind-paw prints were selected for analysis. Stride length was measured as the distance between two successive placements of the same hind paw. The coordination index was defined as the distance between the centers of the ipsilateral forepaw and hind-paw prints, representing interlimb coordination. The mean value of each parameter was calculated for statistical analysis.

2.7 Electrophysiological Evaluation

A Bio-Signal Acquisition and Processing System (BL-420N, Chengdu Taimeng Technology Co., Ltd.; Chengdu, Sichuan, China) was used to perform Hoffmann-reflex (H-reflex) recording and analysis. After anesthetization with 3% isoflurane in 97% oxygen, the left sciatic nerve was exposed by blunt dissection and secured on a bipolar hook electrode. To prevent nerve desiccation during the procedure, oleovitamin was applied to the exposed nerve. Electromyographic (EMG) signals were collected using stainless-steel needle electrodes inserted into the interosseous muscles of the left hind paw, and a ground electrode was placed subcutaneously in the tail.

The H-reflex was elicited by applying single biphasic pulses (100 µs width) to the left sciatic nerve through an isolated pulse stimulator. Both M-waves and H-waves were recorded at varying stimulus intensities to determine the thresholds of motor (MT) and H-reflex. To assess frequency-dependent depression (FDD), stimuli of identical intensity (eliciting Hmax) were delivered at frequencies 0.3 Hz, 5 Hz, and 10 Hz [25]. Subsequently, the variations in the amplitude of the H-reflex at 5 Hz and 10 Hz were expressed as a percentage of the response at 0.3 Hz. A repeated 0.3 Hz stimulation was applied at the end of the recording to confirm that the M-wave remained within 95% of baseline; data were excluded if this criterion was not met. All H-reflex and M-wave measurements, including FDD, were obtained 15 min after the final treatment.

2.8 2,3,5-triphenyl Tetrazolium Chloride (TTC) Staining

The rats were euthanized by cervical dislocation under deep anesthesia induced by intraperitoneal injection of pentobarbital sodium (100 mg/kg body weight, Sigma-Aldrich, St. Louis, MO, USA; Cat. No.: P3761) after the final interventions, and the whole brains were rapidly removed and cooled at –20 °C for approximately 30 min to facilitate sectioning. Each brain was sliced into 2-mm coronal sections and incubated in 0.3% TTC solution (cat. no. SL7140; Coolaber; Beijing, China) at 37 °C in the dark for 20–30 min. The stained slices were then stored in 4% paraformaldehyde (cat. no. SL1830; Coolaber) overnight. Digital images of the brain sections were captured, and infarct areas were analyzed and detected as previously described utilizing ImageJ software (Fiji; National Institutes of Health; Bethesda, MD, USA) [18].

2.9 Immunofluorescence

The embedded lumbar-spinal-cord-enlargement tissue was sectioned into 10 µm slices using a motorized cryostat. Donkey serum was used to block first, and then the following primary antibodies were used: anti-c-Fos (1:500, cat. no. 2250T; Cell Signaling Technology; Danvers, MA, USA), anti-NMDAR1 (1:500, cat. no. ab109182; Abcam; Cambridge, Cambs, UK), and anti-KCC2 (1:500, cat. no. ab259969; Abcam) were incubated overnight at 4 °C. The next day, sections were incubated for 2 h at 37 °C in the dark with the fluorescence antibodies (1:500, cat. no. RGAR002, cat. no. RGAR004; Proteintech; Rosemont, IL, USA). After washing, the sections were mounted with anti-fade mounting medium containing 4′,6-diamidino-2-phenylindole (DAPI) (cat. no. S2110; Solarbio; Beijing, China) and then photographed.

Low-magnification images (4× objective) were captured using an upright fluorescence microscope (Olympus BX43; Tokyo, Japan), and high-resolution images at 10×, 20×, and 40× magnification were acquired with a laser scanning confocal microscope (Olympus FV3000). The number of c-Fos-positive cells in the ventral horn was manually counted, and the mean fluorescence intensity of NMDAR1 in the same region was measured. The expression of KCC2 in the ventral horn was quantified using the previously described method [26].

2.10 Quantitative Real-Time Polymerase Chain Reaction (RT-qPCR)

Total RNA was isolated from the lumbar spinal ventral horn of each rat according to the manufacturer's instructions (cat. no. DP451; Tiangen; Beijing, China). RT-qPCR was performed by mixing cDNA templates with gene-specific primers and PowerUp SYBR Green Master Mix (cat. no. A25742; Thermo Fisher Scientific; Waltham, MA, USA), followed by amplification using a StepOne Plus Real-Time PCR Detection System (CFX Connect; Applied Biosystems; Foster City, CA, USA). The thermal cycling condi-

tions were as follows: initial denaturation at 95 °C for 3 min, followed by 39 cycles of 95 °C for 10 s and 59 °C for 60 s. β-Actin served as the internal control, and relative gene expression was quantified using the $2^{-\Delta\Delta Ct}$ method. Primer sequences are provided in **Supplementary Table 2**.

2.11 Western Blot

Proteins were extracted from the lumbar spinal ventral horn and concentrations were determined with a BCA kit (cat. no. AR0146; Boster; Wuhan, Hubei, China). After SDS-PAGE (8 and 10%) and PVDF membrane transfer (cat. no. IPVH00010; Millipore; Burlington, MA, USA), membranes were blocked and incubated with the following primary antibodies: anti-NMDAR1 (1:6000, cat. no. ab109182; Abcam), anti-KCC2 (1:10,000, cat. no. ab259969; Abcam), anti-phospho-KCC2 (Ser940) (1:3000, cat. no. CAY-29291-100; Cayman Chemical; Ann Arbor, MI, USA), anti-PP1Cγ (1:2000, cat. no. bs-5422R; Bioss; Beijing, China), anti-PP2Aα (1:2000, cat. no. 13482-1-AP; Proteintech), anti-Calpain1 (1:2000; WL03987; Wanleibio; Shenyang, Liaoning, China), anti-SPTAN1 (1:2000, cat. no. 31676-1-AP; Proteintech), and anti-β-actin (1:10,000, cat. no. 66009-1-Ig; Proteintech). Signals were imaged with the CFX Connect Real-Time System (Bio-Rad; Hercules, CA, USA). Semi-quantitative assessment of protein expression was conducted via densitometry using ImageJ (Fiji; National Institutes of Health).

2.12 Data Analysis and Statistical Tests

The data analyses of this study were conducted using SPSS Statistics 25.0 (IBM; Armonk, NY, USA) and GraphPad Prism 10 (GraphPad Software; San Diego, CA, USA). One-way ANOVA, two-way ANOVA, and two-way repeated measures ANOVA were performed as appropriate to assess the significance. Data are presented as mean $\pm$ standard deviation (SD), and differences were considered statistically significant at $p < 0.05$.

3. Results

3.1 Acupuncture Alleviates Spasticity and Enhances Motor Function in MCAO Rats With PSSH

Neurobehavioral tests were conducted to assess the therapeutic effects of acupuncture on PSSH. To evaluate the impact of acupuncture on neurological deficits, the mNSS was assessed on day 3 and day 10 post-MCAO. All rats had an mNSS score of 0 prior to surgery. On day 3 after surgery, compared to sham-operated rats, MCAO surgery induced neurological impairments manifested by significantly elevated mNSS scores (all $p < 0.001$) (Fig. 1D). There were effects of time ($F[2,108] = 2154$, $p < 0.001$), group ($F[3,108] = 934.1$, $p < 0.001$), and their interaction ($F[6,108] = 257.4$, $p < 0.001$). After the intervention, the mNSS scores in the Acup group markedly decreased by day 10 and were lower than those in the Model and CP group (all $p < 0.001$; Fig. 1D). In contrast, no meaningful difference was observed between the Model and CP groups on day 10 ($p > 0.05$; Fig. 1D). These results indicate that acupuncture promoted recovery of neurological function following stroke.

To assess the role of acupuncture on spasticity, the MAS scores of the affected hind limb were measured daily for 10 consecutive days after surgery. All rats had a MAS score of 0 before surgery. Starting from postoperative day 2, the MAS scores of rats in the three MCAO groups markedly increased, but did not in the sham rats ($p < 0.001$) indicating successful induction of spastic hypertonia by MCAO (Fig. 1E). Significant main effects of time ($F[10,396] = 82.92$, $p < 0.001$), group ($F[3,396] = 326.8$, $p < 0.001$), and their interaction ($F[30,396] = 14.13$, $p < 0.001$) were observed. During the treatment period, acupuncture caused a decrease in the MAS scores. From day 7 post-operation onward, the MAS scores in the Acup group were significantly lower than those in the Model group ($p < 0.001$) and the CP group ($p < 0.01$; Fig. 1E). This difference persisted until day 10 post-operation (all $p < 0.001$; Fig. 1E). No significant differences existed between the Model and CP groups at any time (all $p > 0.05$; Fig. 1E). These results suggested that acupuncture effectively alleviated MCAO induced spasticity.

Building on the results of subjective behavioral assessments, we subsequently performed footprint analysis to objectively evaluate motor function in rats (Fig. 1H). On postoperative day 3, MCAO rats in the three surgery groups showed shorter stride lengths of the hind limb than did the sham-operated rats (all $p < 0.001$) and an increased limb-coordination index (all $p < 0.001$; Fig. 1F,G), indicating significant motor impairment induced by MCAO (Fig. 1F,G). By day 10 post-MCAO, the Acup group showed a longer stride length than did either the Model or CP groups (both $p < 0.001$), with no difference between the latter two groups ($p > 0.05$; Fig. 1F). Additionally, no meaningful differences in the limb coordination index were detected among the three surgery groups (all $p > 0.05$; Fig. 1G). These findings suggested that acupuncture intervention promoted motor recovery after stroke, primarily by improving stride characteristics.

3.2 Acupuncture Reduces Spinal Hyperexcitability and Brain Infarct Area in MCAO Rats With PSSH

We assessed the impact of acupuncture on spinal hyperexcitability and ischemic brain damage. The H-reflex is widely used to assess α-motoneuron excitability and the monosynaptic transmission from Ia afferents under spastic conditions [27]. **Supplementary Table 3** summarizes the basic characteristics of M-wave and H-wave responses. No significant differences were detected among these groups on most parameters, except for Mmax and Hmax (all $p > 0.05$). To further quantify reflex excitability, as shown in Fig. 2A, the Hmax/Mmax ratio was larger in the Model group than in the Sham-operated group ($p < 0.001$), indicat-

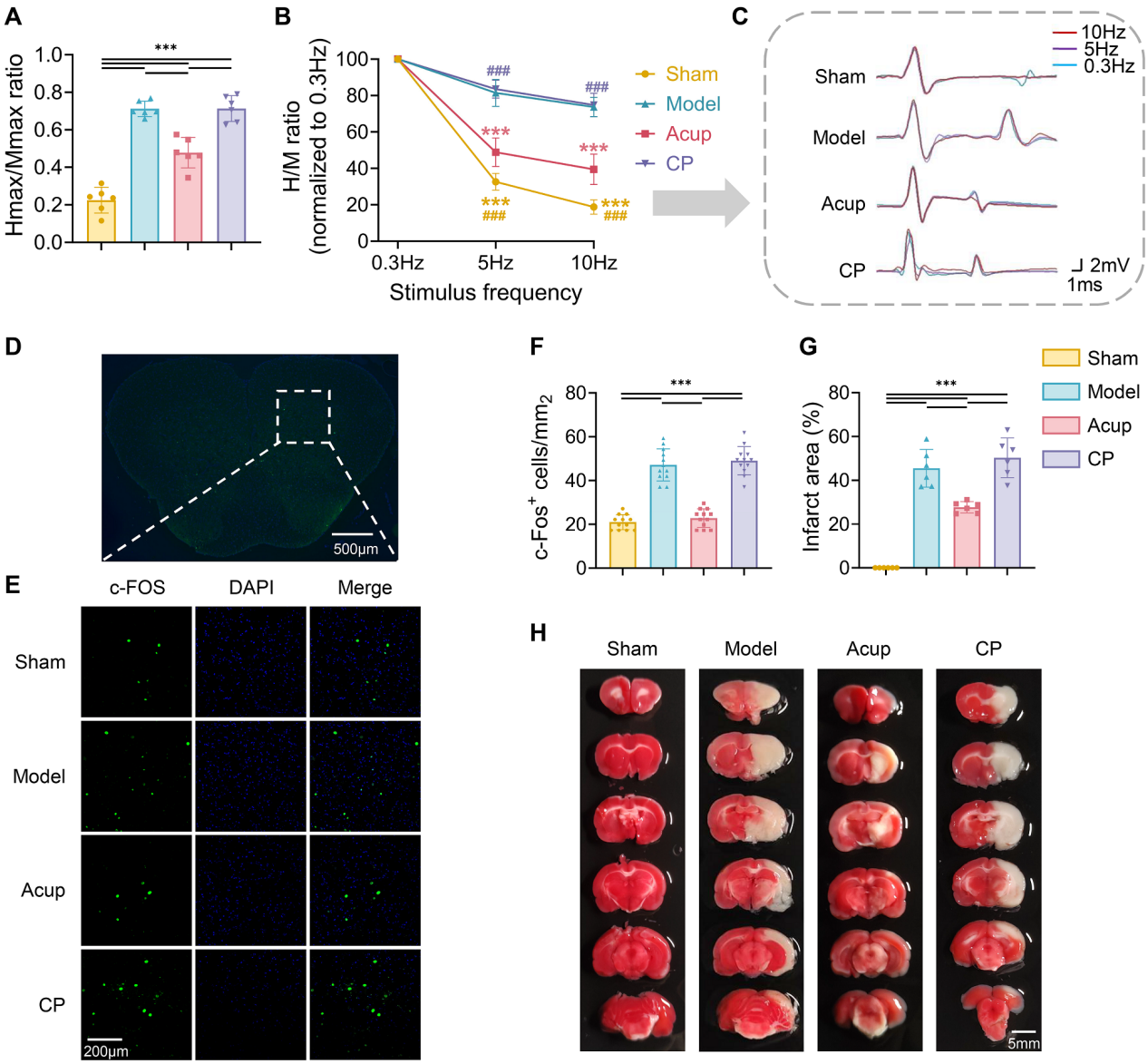

Fig. 2. Acupuncture mitigates MCAO-induced spinal hyperexcitability and ischemic brain injury. (A) Hmax/Mmax ratio was measured to assess spinal excitability (N = 6). (B) FDD of the H-reflex (N = 6). (C) Representative H-reflex traces recorded at 0.3 Hz (blue), 5 Hz (purple), and 10 Hz (red) to show changes in the H-reflex (N = 6). (D) Distribution of c-Fos in the lumbar spinal ventral horn neurons. Scale bar, 500 μm. (E) Representative images of c-Fos expression in the lumbar spinal ventral horn of each group. Scale bar, 200 μm. (F) Analysis of c-Fos-positive cell density (cells per mm^2) (12 spinal slices from 4 rats per group). (G,H) TTC staining and quantitative analysis of infarction areas in the brain (N = 6). Scale bar, 5 mm. Data are presented as mean ± SD. $^{♦♦♦}p < 0.001$ compared to the Model group; $^{###}p < 0.001$ compared to the Acup group; $^{***}p < 0.001$. H/M ratio, Hmax/Mmax ratio; FDD, frequency-dependent depression.

ing enhanced spinal excitability after stroke. Acupuncture treatment at GB34 significantly decreased the Hmax/Mmax ratio ($p < 0.001$), whereas needle manipulation at the control point did not show such an effect ($p > 0.05$; Fig. 2A). These results suggested that acupuncture effectively suppressed spinal hyperexcitability after stroke.

Subsequently, FDD was measured to evaluate spinal reflex activity in MCAO rats. Impaired FDD is widely recognized as a hallmark of spinal hyperreflexia [28]. We evoked H-reflexes at stimulation frequencies of 0.3 Hz, 5 Hz, and 10 Hz to evaluate the extent of FDD. The results showed a frequency-dependent decline in H-reflex amplitude across all groups, indicating the presence of FDD to varying degrees (Fig. 2B,C). Significant effects were observed for stimulation frequency ($F[2,60] = 588.7$, $p < 0.001$), group ($F[3,60] = 206.9$, $p < 0.001$), and their in-

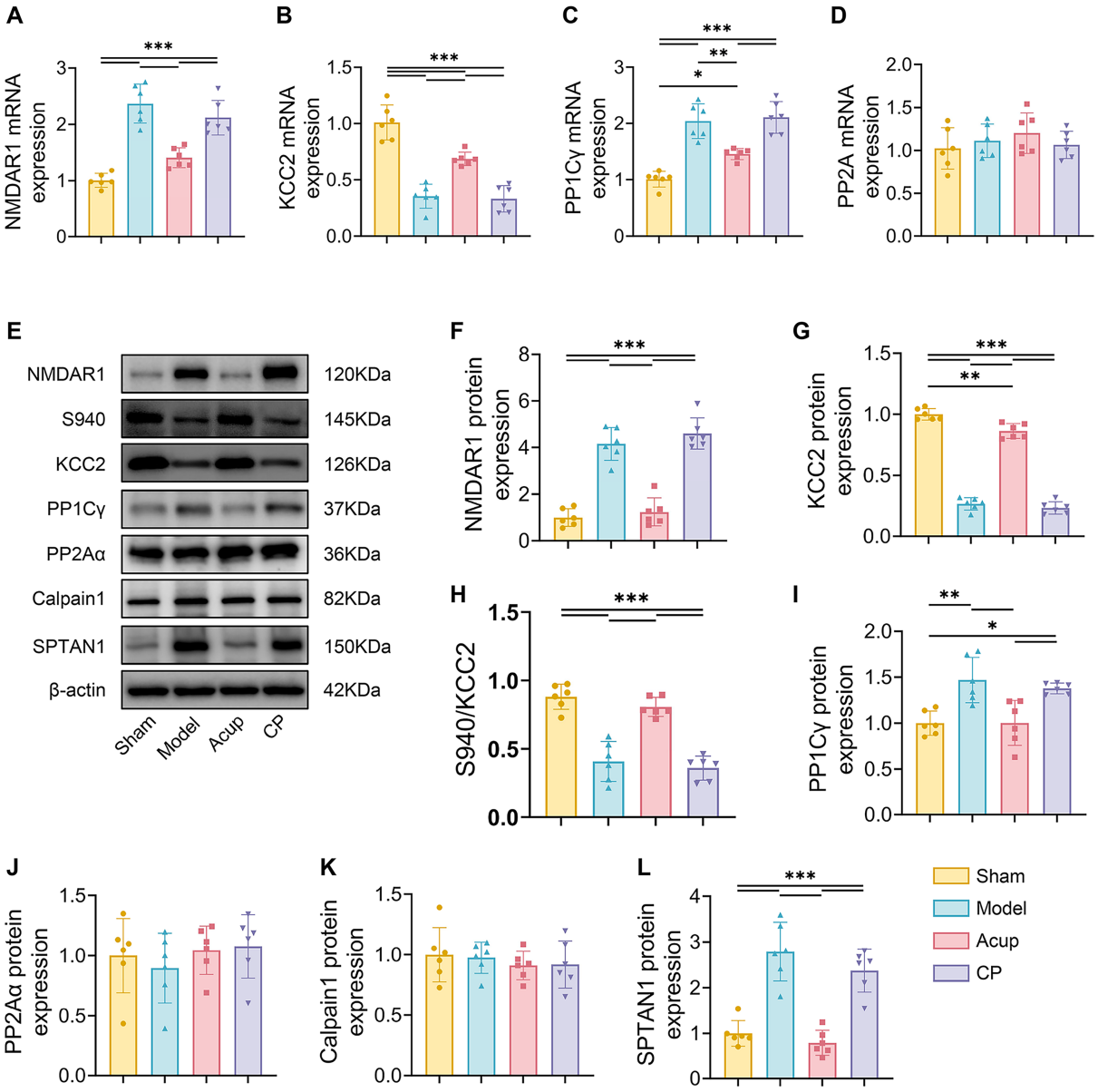

Fig. 3. Acupuncture downregulates the expression of NMDAR1 and restores KCC2 expression and activation in spinal cord of MCAO rats with PSSH. (A–D): The mRNA expressions of *NMDAR1* (A), *KCC2* (B), *PP1Cγ* (C) and *PP2A* (D) were detected by RT-qPCR. (E) Representative Western blot images showing the expression of NMDAR1, S940, KCC2, PP1Cγ, PP2Aα, calpain1, and SPTAN1. (F–J): Quantitative analysis of expressions of NMDAR1 (F), KCC2 (G), S940/KCC2 (H), PP1Cγ (I), PP2Aα (J), calpain1 (K) and SPTAN1 (L) by using Western blot. N = 6 per group. Data are presented as mean ± SD. *$p < 0.05$, **$p < 0.01$, ***$p < 0.001$. NMDAR1, N-methyl-D-aspartate receptor 1; KCC2, potassium-chloride cotransporter 2; S940, serine940; SPTAN1, nonerythroid spectrin αII; PP2A, protein phosphatase 2A.

teraction (F[6,60] = 52.14, $p < 0.001$). Further analysis demonstrated that at both 5 Hz and 10 Hz, the Acup group exhibited greater depression of the H-reflex than did the Model group ($p < 0.001$), whereas the CP group FDD was not different from that of the Model group ($p > 0.05$; Fig. 2B). These findings suggested that acupuncture at GB34 partially restored FDD and enhanced spinal-reflex modulation after stroke.

As a cellular marker of neuronal activation, c-Fos expression in spinal-ventral-horn neurons was analyzed to further verify the modulatory effect of acupuncture on neuronal excitability (Fig. 2D,E). The c-Fos-positive neuron count was higher in model rats than in sham-operated rats ($p < 0.001$; Fig. 2F). Compared with Model group, acupuncture exerted substantial reduction of the c-Fos-positive neuron count ($p < 0.001$), whereas no similar changes were observed in CP group ($p > 0.05$; Fig. 2F). These findings sug-

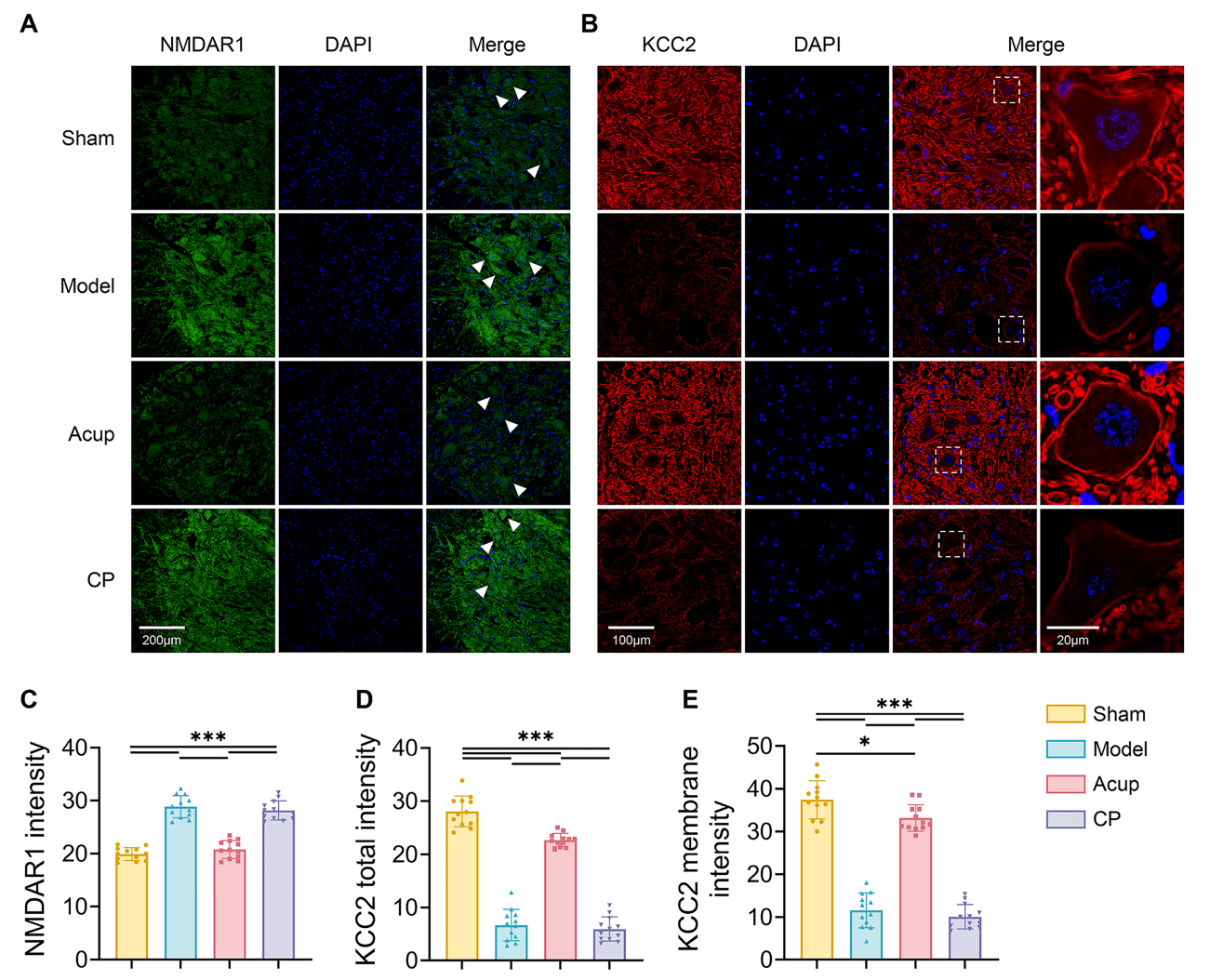

Fig. 4. Acupuncture downregulates the expression of NMDAR1 in spinal ventral horn and upregulates the total and membrane expression of KCC2 in spinal motor neuros. (A,B) Representative immunofluorescence images indicating NMDAR1 (A, green), KCC2 (B, red) co-localization with all nuclei of cells stained by DAPI (blue) in the lumbar spinal ventral horn. Scale bar, 200 μm, 100 μm, 20 μm. The white arrows indicate representative individual neurons, and the white boxes indicate regions of interest, which are enlarged and shown adjacent to the original image. (C–E) Mean fluorescence intensity of NMDAR1 (C), KCC2 total intensity (D) and KCC2 membrane intensity (E) were expressed as the ratio of integrated density to the observation fields. 12 spinal slices from 4 rats per group. Data are presented as mean ± SD. *$p < 0.05$, ***$p < 0.001$. DAPI, 4′,6-Diamidino-2-phenylindole.

gested that acupuncture at GB34 effectively suppressed hyperexcitability in the spinal ventral horn induced by stroke.

TTC staining was used to evaluate ischemic brain injury. As depicted in Fig. 2G, no obvious infarct area was observed in the Sham group, whereas all three surgery groups exhibited clear ischemic regions, confirming successful induction of cerebral infarction by MCAO. After intervention, the infarct area in the Acup group was smaller than that in the Model group ($p < 0.001$), suggesting that acupuncture mitigated ischemic brain damage (Fig. 2H). No significant difference was observed between the Model and the CP group ($p > 0.05$; Fig. 2H).

3.3 Acupuncture Downregulates NMDAR1 and Restores KCC2 Expression and Activation in MCAO Rats With PSSH

NMDAR enhances neuronal excitability primarily by mediating Ca^{2+} influx, whereas KCC2 maintains low intracellular Cl^- levels to support GABAergic inhibition. Both play critical roles in regulating neuronal excitability. We investigated whether acupuncture treatment alleviated PSSH by modulating NMDAR and KCC2 expression in the spinal ventral horn. NMDAR1 is involved in Ca^{2+} influx and regulating neuronal excitability [29]. We assessed NMDAR1 expression in the spinal ventral horn. The results showed that NMDAR1 mRNA and protein expression levels were higher in the Model group than in the Sham group

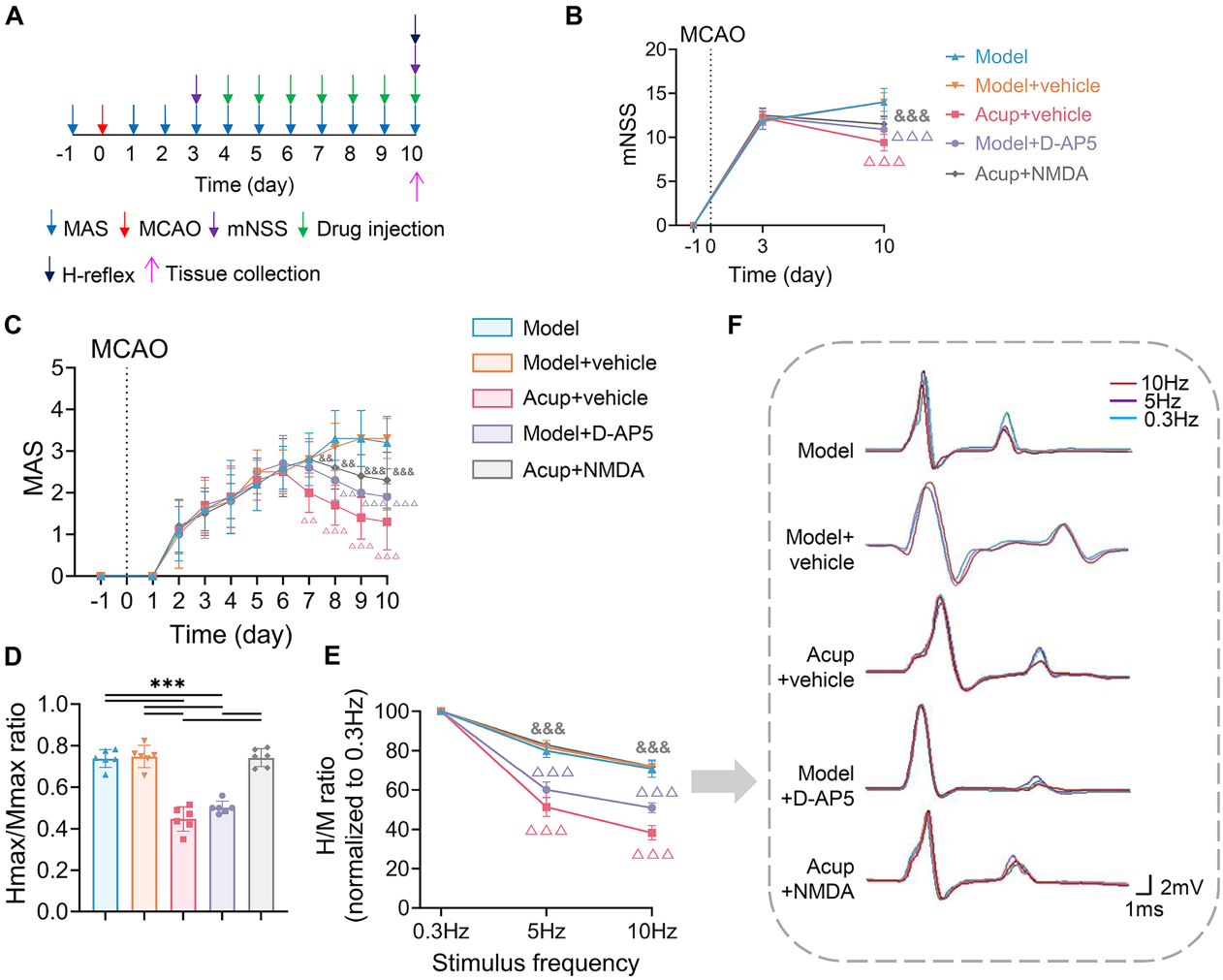

Fig. 5. The impact of NMDAR antagonist and agonist on acupuncture effects on neurological deficits, spasticity, and H-reflex in MCAO rats with PSSH. (A) Timeline of experimental procedures. (B) Neurological deficits assessed by the mNSS (N = 10). (C) Muscle tone assessed by the MAS (N = 10). (D) Hmax/Mmax ratio was measured to assess spinal excitability (N = 6). (E) FDD of the H-reflex (N = 6). (F) Representative H-reflex traces recorded at 0.3 Hz (blue), 5 Hz (purple), and 10 Hz (red) to show changes in the H-reflex. Data are presented as mean ± SD. $^{\triangle\triangle}p < 0.01$, $^{\triangle\triangle\triangle}p < 0.001$ compared to the Model + vehicle group; $^{\&\&}p < 0.01$, $^{\&\&\&}p < 0.001$ compared to the Acup + vehicle group; $^{***}p < 0.001$.

(all $p < 0.001$; Fig. 3A,E,F; Fig. 4A,C). After acupuncture treatment, NMDAR1 expression was markedly lower in the Acup group than in the Model group (all $p < 0.001$), suggesting that acupuncture effectively inhibited NMDAR1 expression after stroke (Fig. 3A,E,F; Fig. 4A,C).

Then we evaluated KCC2 expression in the spinal ventral horn. The results consistently indicated that both KCC2 mRNA levels and total protein expression were lower in the Model group than in the Sham group (all $p < 0.001$), whereas acupuncture markedly restored KCC2 expression in the Acup group (all $p < 0.001$; Fig. 3B,E,G; Fig. 4B,D). We further examined the phosphorylation level at Ser940 and assessed KCC2 membrane localization. The results showed that both Ser940 phosphorylation and membrane-associated KCC2 expression were lower in the Model group than in the Sham group, and acupuncture treatment significantly reversed these impairments (all $p < 0.001$; Fig. 3E,H; Fig. 4E). These findings suggested that acupuncture upregulated KCC2 total expression and promoted its functional recovery by enhancing Ser940 phosphorylation and increasing membrane localization. Collectively, these results suggested that acupuncture attenuated neuronal hyperexcitability in the spinal ventral horn by downregulating NMDAR1 and restoring KCC2 expression and activity, thereby contributing to its therapeutic effects on PSSH.

We further explored the potential mechanisms by which NMDAR suppresses KCC2 expression and activity. Phosphorylation at the Ser940 site is primarily dephosphorylated by PP1 and protein phosphatase 2A (PP2A). We assessed the expression of PP1Cγ and PP2Aα, the cat-

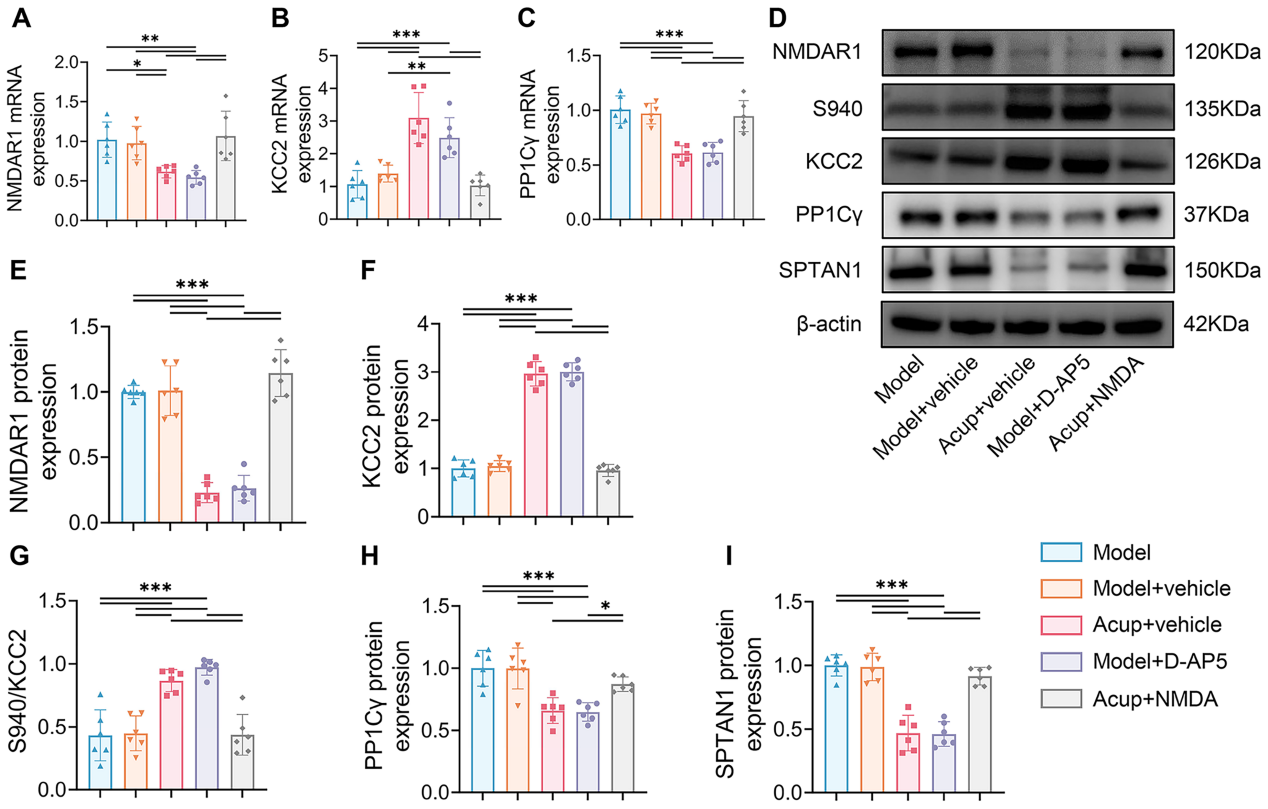

Fig. 6. The effects of NMDAR antagonist and agonist on the NMDAR-PP1/Calpain1-KCC2 pathway. (A–C) The mRNA expressions of *NMDAR1* (A), *KCC2* (B) and *PP1Cγ* (C) were detected by RT-qPCR. (D) Representative Western blot images showing the expression of NMDAR1, S940, KCC2, PP1Cγ and SPTAN1. (E–I): Quantitative analysis of expressions of NMDAR1 (E), KCC2 (F), S940/KCC2 (G), PP1Cγ (H) and SPTAN1 (I) by using Western blot. N = 6 per group. Data are presented as mean ± SD. *$p < 0.05$, **$p < 0.01$, ***$p < 0.001$.

alytic subunits of PP1 and PP2A, in the spinal ventral horn [30,31]. The results showed that, compared with the Sham group, the Model group exhibited elevated mRNA and protein levels of PP1Cγ (both $p < 0.01$), whereas acupuncture markedly downregulated its expression (both $p < 0.01$; Fig. 3C,E,I). In contrast, no differences were observed in the mRNA of PP2A and protein levels of PP2Aα among the groups (all $p > 0.05$; Fig. 3D,E,J). These findings suggested that acupuncture promoted KCC2 activity by inhibiting PP1-mediated Ser940 dephosphorylation.

Dephosphorylation of KCC2 at the Ser940 site leads to its inactivation and internalization, followed by degradation by calpain1 in the cytoplasm. The activity of calpain1 is highly dependent on NMDAR-mediated Ca^{2+} influx [32,33]. Nonerythroid spectrin αII (SPTAN1) is a classical substrate of calpain1; it is cleaved into a stable 150-kDa fragment, and is commonly used as a marker of calpain1 activity [32]. We measured the levels of calpain1 and SPTAN1 in the spinal ventral horn. As shown in Fig. 3L, the protein level of SPTAN1 was higher after MCAO ($p < 0.001$) than in sham rats, and acupuncture evidently inhibited this elevation ($p < 0.001$). However, calpain1 protein expression did not differ markedly among all groups ($p > 0.05$; Fig. 3E,K). These findings suggested that acupuncture may have inhibited calpain1 activity, rather than affecting its expression, thereby reducing KCC2 degradation and promoting its expression. All original WB figures in Fig. 3 are provided in the **Supplementary Material-Uncut western bloting images**.

3.4 NMDAR Interferes With the Effects of Acupuncture on Pssh and NMDAR- PP1/Calpain1-KCC2 Pathway

NMDAR directly enhances neuronal excitability by mediating Ca^{2+} influx and downregulates the expression and activity of KCC2, thereby indirectly weakening inhibitory regulation. Given that acupuncture has been shown to alleviate PSSH by modulating KCC2, we further investigated whether this effect was associated with its regulation of NMDAR1. To this end, the NMDAR agonist NMDA and antagonist D-AP5 were administered intrathecally. We evaluated mNSS scores, MAS scores, and H-reflex parameters in each group. After treatment, the Acup + NMDA group showed significantly higher mNSS and MAS scores, a higher Hmax/Mmax ratio, and lower FDD suppression than did the Acup + Vehicle group (all $p < 0.001$), indi-

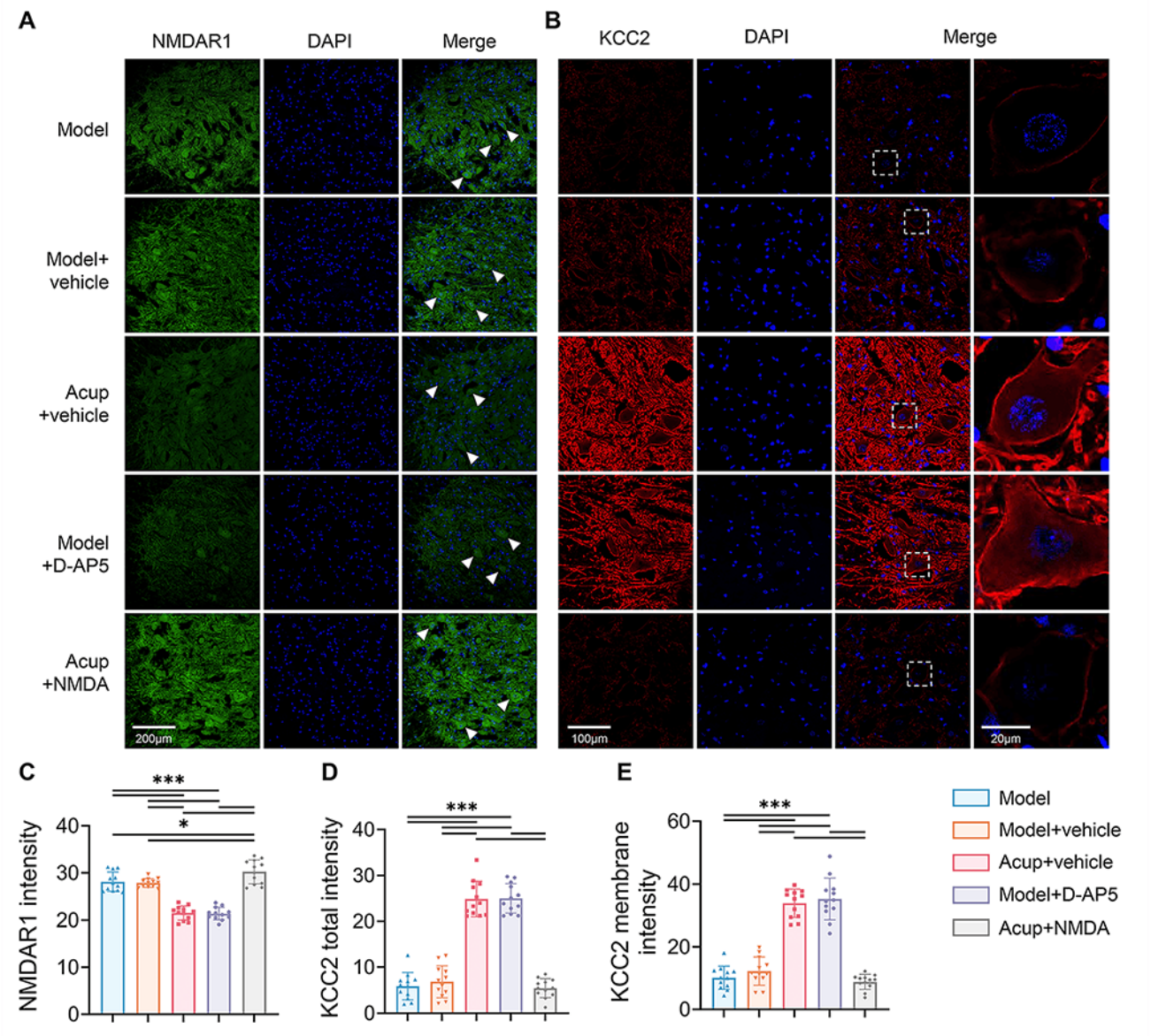

Fig. 7. The effects of NMDAR antagonist and agonist on the expression of NMDAR1 in spinal ventral horn and the total and membrane expression of KCC2 in spinal motor neuros. (A,B) Representative immunofluorescence images indicating NMDAR1 (A, green), KCC2 (B, red) co-localization with all nuclei of cells stained by DAPI (blue) in the lumbar spinal ventral horn. Scale bar, 200 μm, 100 μm, 20 μm. The white arrows indicate representative individual neurons, and the white boxes indicate regions of interest, which are enlarged and shown adjacent to the original image. (C–E) Mean fluorescence intensity of NMDAR1 (C), KCC2 total intensity (D) and KCC2 membrane intensity (E) were expressed as the ratio of integrated density to the observation fields. 12 spinal slices from 4 rats per group. Data are presented as mean ± SD. *$p < 0.05$, ***$p < 0.001$. D-AP5, D-(-)-2-Amino-5-phosphonopentanoic acid.

cating that NMDAR activation diminished the therapeutic effects of acupuncture (Fig. 5B–F). In contrast, the Model + D-AP5 group exhibited significant improvements in behavioral and electrophysiological outcomes (all $p < 0.001$), suggesting that NMDAR inhibition alleviated neurological deficits and spasticity, and reduced spinal motor-neuron excitability (Fig. 5B–F). Additionally, no significant intergroup variation was observed between the Model group and the Model + Vehicle group, suggesting that the vehicle did not interfere with the results (all $p > 0.05$; Fig. 5B–F).

To verify the effectiveness of the pharmacological intervention in modulating NMDAR1, we examined NMDAR1 expression in the spinal ventral horn. Results showed that NMDAR1 mRNA and protein levels were evidently lower in the Model + D-AP5 group than in the Model + Vehicle group (all $p < 0.01$), whereas they were significantly higher in the Acup + NMDA group than in the Acup + Vehicle group (all $p < 0.01$; Fig. 6A,D,E; Fig. 7A,C). No significant intergroup variation was observed between the Model group and the Model + Vehicle group (all $p > 0.05$;

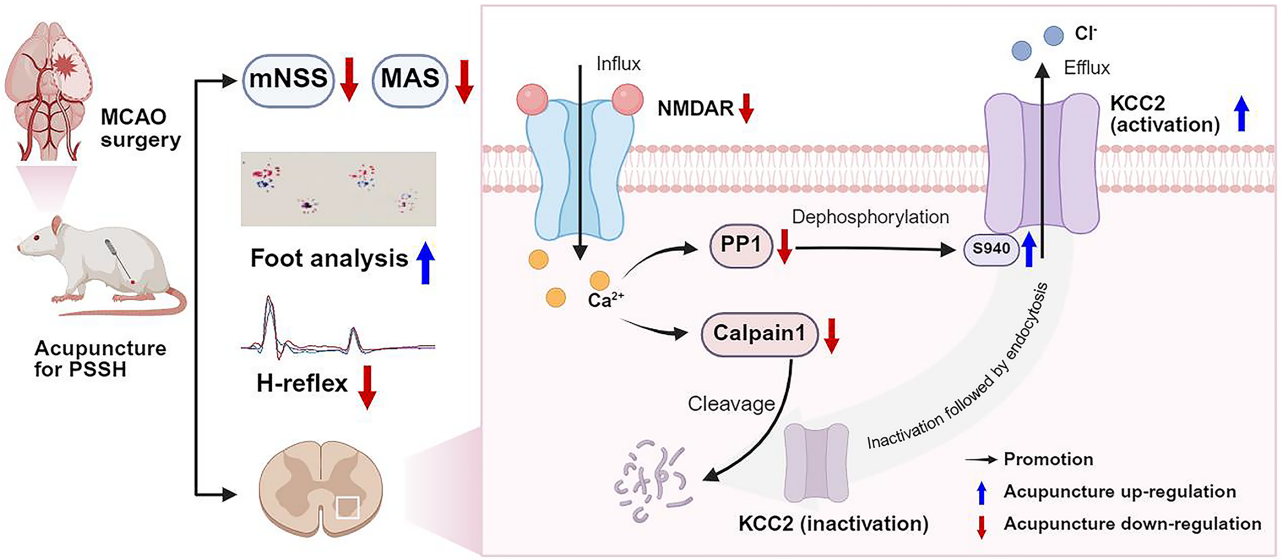

Fig. 8. Acupuncture alleviates PSSH via modulating the NMDAR-PP1/Calpain1-KCC2 pathway in spinal cord (Created with BioRender.com).

Fig. 6A,D,E; Fig. 7A,C). These findings confirmed that the pharmacological agents effectively modulated NMDAR1 expression and that the vehicle did not interfere with the results. We next assessed the expression and activity of KCC2 in the spinal ventral horn. The Acup + NMDA group exhibited significantly lower KCC2 mRNA levels, total protein expression, Ser940 phosphorylation, and membrane expression than did the Acup + Vehicle group (all $p < 0.001$), indicating that NMDAR activation attenuated the upregulation of KCC2 by acupuncture (Fig. 6B,D,F,G; Fig. 7B,D,E). Conversely, all of these measures were higher in the Model + D-AP5 group than in the Model + Vehicle group (all $p < 0.01$), suggesting that NMDAR inhibition facilitated the restoration of KCC2 expression and activity after stroke (Fig. 6B,D,F,G; Fig. 7B,D,E). Taken together, these findings suggested that NMDAR modulation was closely associated with the effect of acupuncture on PSSH by upregulating KCC2.

We next determined whether the process by which acupuncture promoted KCC2 activity by inhibiting PP1-mediated Ser940 dephosphorylation was associated with the regulation of NMDAR. The Acup + NMDA group exhibited higher PP1Cγ mRNA and protein levels than did the Acup + Vehicle group (both $p < 0.05$), whereas the Model + D-AP5 group showed lower levels of expression of PP1Cγ than did the Model + Vehicle group (both $p < 0.001$; Fig. 6C,D,H). These results suggested that acupuncture maintained KCC2 activity by suppressing NMDAR-induced upregulation of PP1.

We further clarified whether the process by which acupuncture inhibited calpain1 to reduce KCC2 degradation was associated with the regulation of NMDAR1 by acupuncture. SPTAN1 expression was substantially higher in the Acup + NMDA group than in the Acup + Vehicle group ($p < 0.001$), whereas it was lower in the Model + D-AP5 group than in the Model + Vehicle group ($p < 0.001$; Fig. 6D,I). These data causally suggested that acupuncture enhanced the protein stability of KCC2 by suppressing NMDAR-mediated activation of calpain1. All original WB figures in Fig. 6 are provided in the **Supplementary Material-Raw data**.

4. Discussion

This study identified a potential mechanism underlying the therapeutic effects of acupuncture treatment on PSSH. Our results demonstrated that acupuncture treatment significantly alleviated spasticity and improved motor function in MCAO rats with PSSH. Acupuncture appears to exert its therapeutic effects by modulating the NMDAR-PP1/Calpain1-KCC2 pathway, which regulates the excitability of spinal ventral-horn neurons. The effects of pharmacological manipulation using the NMDAR agonist NMDA and antagonist D-AP5 further supported the critical involvement of NMDAR in the effects of acupuncture (Fig. 8).

PSSH is a common sequela of stroke, with a reported incidence of up to 39.5% [34]. It is characterized by increased muscle tone and spastic movement patterns, which impede motor recovery and reduce quality of life [35]. To replicate the pathological features of PSSH and evaluate the efficacy of acupuncture treatment, we used the well-established MCAO model in rats and selected GB34 as

the intervention site. Located anteroinferior to the fibular head, GB34 corresponds segmentally to the lumbar-spinal-cord enlargement that governs lower limb motor control, and its efficacy in treating PSSH has been well documented [18,36]. We assessed muscle tone in the affected hind limb using the MAS scores and conducted footprint analysis to evaluate motor performance quantitatively. Given that the regulation of movement also depends on sensory input and central integration, we used the mNSS scores to assess the overall degree of neurological impairment. Acupuncture at GB34 effectively reduced spasticity, improved motor function, and facilitated the recovery of overall neurological function in MCAO rats.

Spasticity after stroke is primarily attributed to disrupted supraspinal inhibition of spinal reflex circuits. Specifically, damage to upper motor neurons leads to a loss of descending inhibitory control, resulting in hyperexcitability of spinal stretch reflexes and consequent pathological increases in muscle tone [37]. As the convergence site of motor neurons, spinal ventral-horn hyperexcitability directly contributes to sustained muscle contractions, ultimately driving spasticity and motor impairment [38]. The H-reflex serves as a classical electrophysiological index of spinal excitability. In our study, MCAO rats exhibited a significantly increased Hmax/Mmax ratio and reduced FDD, indicating enhanced excitability of spinal reflexes. These results were consistent with previous findings in both spinal cord injury and MCAO models [18,25]. Acupuncture intervention effectively reversed these abnormalities. Building on these observations, we further examined the expression of c-Fos in spinal ventral-horn neurons. The classical immediate early gene c-Fos is widely used as a molecular marker of neuronal activation. Elevated c-Fos expression in spasticity models induced by photothrombosis has been reported [39]. Our results revealed a marked increase in the number of c-Fos-positive neurons in the spinal ventral horn of MCAO rats; this number was significantly reduced by acupuncture. This result reinforced our electrophysiological findings, providing further evidence that acupuncture treatment mitigated spinal ventral-horn hyperexcitability.

We focused on the critical role of the NMDAR-PP1/Calpain1-KCC2 pathway in regulating neuronal excitability. NMDAR, an ionotropic glutamate receptor with high Ca^{2+} permeability, is widely expressed on motor neurons within the spinal ventral horn. Sustained activation of NMDAR can lead to neuronal hyperexcitability and trigger multiple downstream signaling cascades [8]. In addition to motor neurons, the ventral horn also contains GABAergic inhibitory interneurons, which regulate motor neuron activity [40,41]. KCC2 is a key molecular determinant of GABAergic inhibition, which maintains a low intracellular Cl^- concentration required for $GABA_A$ receptor-mediated hyperpolarization [9,10]. Previous research has reported that KCC2 expression in the lumbar enlargement is markedly reduced after stroke, and acupuncture treatment can restore GABAergic inhibition and reduce neuronal excitability by upregulating KCC2 expression. This effect was abolished by the KCC2 antagonist D-Indo-oxy-5-sulfonic acid [18]. We further demonstrated that stroke upregulated NMDAR1 expression and induced a significant reduction in total KCC2 expression, membrane localization, and phosphorylation at Ser940 in the spinal ventral horn. Acupuncture treatment ameliorated these pathological changes. Importantly, the protective effect of acupuncture on KCC2 was impeded by NMDAR, but was restored by D-AP5, suggesting that this effect may involve suppression of NMDAR expression.

To explore how acupuncture might influence KCC2 regulation, we investigated two key aspects: the activity and protein stability of KCC2. Phosphorylation at the Ser940 site of KCC2 is essential for its membrane transport function and surface stability. In rat hippocampal neurons, excessive glutamate-induced activation of NMDAR has been shown to trigger Ca^{2+} influx, which subsequently activates protein phosphatases to dephosphorylate Ser940 [11]. This process impairs KCC2 function and reduces its membrane localization, thereby reversing $GABA_A$ receptor-mediated hyperpolarization and enhancing neuronal excitability. This process can be blocked by okadaic acid, an inhibitor of PP1 and PP2A. We observed an upregulation of PP1Cγ expression in the spinal ventral horn of MCAO rats. Acupuncture treatment significantly reduced PP1Cγ levels, and this effect was abolished by NMDA, suggesting that acupuncture may have suppressed PP1 activity and preserved KCC2 phosphorylation and function by inhibiting NMDAR-mediated Ca^{2+} influx. In contrast, PP2A remained unchanged. Although PP1 and PP2A share highly conserved catalytic domains and overlapping substrate profiles, their functional divergence depends on their distinct recognition and regulation of short linear motifs (SLiMs) [42]. Based on these observations, we speculated that NMDAR-mediated Ca^{2+} signaling after stroke may have preferentially activated PP1 over PP2A, potentially contributing to KCC2 inactivation. Additionally, we examined potential changes in KCC2 protein stability. Elevated intracellular Ca^{2+} induced by NMDAR activation can also stimulate calpain1, a Ca^{2+}-dependent protease that degrades internalized, non-functional KCC2 in the cytoplasm [33]. In peripheral-nerve-injury models, NMDAR overactivation has been shown to promote calpain1-mediated cleavage of the KCC2 C-terminal domain, a process that can be prevented by D-AP5 [12]. Although we did not observe significant changes in calpain1 expression, the cleavage product of its substrate SPTAN1 was increased, indicating enhanced calpain1 activity. Both acupuncture and D-AP5 significantly reduced SPTAN1 degradation, suggesting that acupuncture may have attenuated calpain1 activity and protected KCC2 from excessive degradation by suppressing NMDAR.

Building upon previous studies on acupuncture for PSSH, the present study systematically investigated how acupuncture treatment alleviates spasticity and promotes motor recovery through modulation of the NMDAR-PP1/Calpain1-KCC2 pathway. Our findings revealed a dual pathological role of NMDAR in promoting neuronal hyperexcitability: by facilitating Ca^{2+} influx that directly enhances neuronal excitation, and by impairing GABAergic inhibition through suppression of KCC2 function. Further analysis demonstrated that NMDAR downregulated KCC2 function through two pathways: upregulation of PP1 leading to Ser940 dephosphorylation, and activation of calpain1 promoting degradation of KCC2. Acupuncture treatment significantly reduced NMDAR1 expression, which was accompanied by a restoration of KCC2 activity and protein stability. Collectively, these effects converged to reduce the hyperexcitability of spinal ventral-horn neurons and contribute to the therapeutic efficacy of acupuncture in PSSH. Additionally, our findings also preliminarily offered a potential for future targeted interventions, particularly the development of pharmacological agents aimed at negatively modulating NMDAR-PP1/Calpain1 pathway to enhance KCC2 activity and stability for stroke-recovery management.

The intervention timing of acupuncture treatment for PSSH is also a critical issue. In this study, continuous acupuncture intervention was administered from day 4 to day 10 after MCAO, primarily based on observations from previous studies indicating that limb spasticity after MCAO begins to manifest on day 3 post-surgery, with a significant increase in MAS scores starting on day 3 and persisting until day 10 post-surgery [18,36,43]. Rats recover more rapidly than do clinical patients, and the period from day 3 to day 10 post-surgery may resemble the spasticity phase observed in clinical stroke patients. Furthermore, given that our primary focus was on observing gross motor function of the lower limbs, our observations were conducted up to day 10 post-surgery. Future studies involving fine motor skills may necessitate longer observation periods.

According to classical acupuncture theory, selecting acupoints and using needling techniques that are appropriate for the specific disease, are key factors in achieving therapeutic efficacy with acupuncture. Although this study was an animal experiment, it demonstrated that when treating lower-limb spastic hemiplegia after stroke, applying a motion-style needling technique (waggle needling) at GB34, which is located on the spastic antagonist muscle, is beneficial for alleviating post-stroke spasticity. Specifically, our findings indicated that future clinical strategies could validate approaches targeting the NMDAR-KCC2 pathway for PSSH.

Despite these insights, there were several limitations. This study primarily focused on the NMDAR-PP1/Calpain1-KCC2 pathway, however, the regulation of KCC2 may vary across different neuronal subtypes, so elucidation may necessitate the use of cell-type-specific markers and *in situ* detection techniques. Given that different NMDAR subunits can exert distinct effects on neuronal excitability, subunit-specific inhibitors or genetic approaches should be used to delineate the specific contributions. Ca^{2+} signaling is a key mediator of excitability regulation, but in the present work, we only observed the cumulative effect of Ca^{2+} influx via c-Fos and calpain1 activation. Future experiments combining Ca^{2+} imaging for real-time recording of neuronal Ca^{2+} dynamics will provide a more precise assessment of excitability changes. In addition, the inclusion of inhibitory synaptic markers would help to characterize how acupuncture modulates neural excitability. Acupuncture signals are primarily transmitted via the spinal dorsal horn; they may modulate ventral-horn motor neurons through local interneuronal networks, or ascend to brainstem or cortical centers and influence spinal excitability via descending pathways [44]. Further research combining viral tracing and multi-site electrophysiological recording would help clarify these cross-structural interactions. To avoid the confound of hormonal effects on neuronal activity, the present study used only male rats. Future work will include females in order to explore potential sex-related differences in the regulation of neuronal excitability by acupuncture. Moreover, to further validate acupoint specificity, more appropriate non-acupoint control sites will be considered. Our study used single-acupoint stimulation to provide mechanistic clarity, which differs from clinical acupuncture practice [45,46]. In addition, we examined only consecutive acupuncture treatments from postoperative day 4 to day 10. Future research could investigate multi-acupoint protocols and varied treatment frequencies or durations to better inform clinical application.

5. Conclusion

This study systematically elucidated the potential mechanism underlying the therapeutic effects of acupuncture treatment in PSSH. Acupuncture effectively modulated the excitability of spinal ventral-horn neurons to ameliorate spasticity and improve motor function in MCAO rats with PSSH. These effects of acupuncture were associated with its modulation of the NMDAR-PP1/Calpain1-KCC2 pathway. Acupuncture treatment suppressed NMDAR expression and upregulated both the expression and function of KCC2, thereby alleviating spinal hyperexcitability after ischemic stroke.

Abbreviations

PSSH, Post-stroke spastic hemiplegia; MCAO, Middle cerebral artery occlusion; KCC2, Potassium-chloride cotransporter 2; NMDAR, N-methyl-d-aspartate receptor; PP1, Protein phosphatase 1; TTC, 2,3,5-triphenyl tetrazolium chloride; RT-qPCR, Quantitative real-time pcr; c-Fos, Immediate early gene c-Fos; GABA, γ-aminobutyric acid; D-AP5, D-(-)-2-Amino-5-phosphonopentanoic acid;

MCA, Middle cerebral artery; CBF, Cerebral blood flow; ROIs, Regions of interest; mNSS, modified Neurological Severity Score; MAS, Modified Ashworth Scale; EMG, Electromyographic; MT, Thresholds of motor; FDD, Frequency dependent depression; DAPI, 4′,6-diamidino-2-phenylindole; PP2A, Protein phosphatase 2A; SPTAN1, Nonerythroid spectrin αII.

Availability of Data and Materials

The data that support the findings of this study are available in the **Supplementary Material** of this article.

Author Contributions

Conceptualization, JLH and LXM; methodology, JLH, YXZ, and JSW; software, JYX, and MYC; validation, JYX; formal analysis, JLH; investigation, YXZ, JSW, and LHM; resources, LXM; data curation, YXZ and MYC; writing—original draft preparation, JLH; writing—review and editing, JLH and LXM; visualization, JLH and JYX; supervision, LHM; project administration, LXM; funding acquisition, LXM. All authors contributed to editorial changes in the manuscript. All authors read and approved the final manuscript. All authors have participated sufficiently in the work and agreed to be accountable for all aspects of the work.

Ethics Approval and Consent to Participate

All animal procedures were performed in accordance with the NIH Guide for the Care and Use of Laboratory Animals and approved by the Ethics Committee for Animal Experimentation of Beijing University of Chinese Medicine (BUCM-2024101002-4017).

Acknowledgment

Not applicable.

Funding

This research was funded by the National Natural Science Foundation of China, grant number 82274655.

Conflict of Interest

The authors declare no conflict of interest.

Supplementary Material

Supplementary material associated with this article can be found, in the online version, at https://doi.org/10.31083/JIN46980.

References

[1] Wieters F, Weiss Lucas C, Gruhn M, Büschges A, Fink GR, Aswendt M. Introduction to spasticity and related mouse models. Experimental Neurology. 2021; 335: 113491. https://doi.org/10.1016/j.expneurol.2020.113491.

[2] Bavikatte G, Subramanian G, Ashford S, Allison R, Hicklin D. Early Identification, Intervention and Management of Post-stroke Spasticity: Expert Consensus Recommendations. Journal of Central Nervous System Disease. 2021; 13: 11795735211036576. https://doi.org/10.1177/11795735211036576.

[3] Marinelli L, Currà A, Trompetto C, Capello E, Serrati C, Fattapposta F, *et al*. Spasticity and spastic dystonia: the two faces of velocity-dependent hypertonia. Journal of Electromyography and Kinesiology: Official Journal of the International Society of Electrophysiological Kinesiology. 2017; 37: 84–89. https://doi.org/10.1016/j.jelekin.2017.09.005.

[4] Urbin MA, Collinger JL, Wittenberg GF. Corticospinal recruitment of spinal motor neurons in human stroke survivors. The Journal of Physiology. 2021; 599: 4357–4373. https://doi.org/10.1113/JP281311.

[5] Madhavan S, Krishnan C, Jayaraman A, Rymer WZ, Stinear JW. Corticospinal tract integrity correlates with knee extensor weakness in chronic stroke survivors. Clinical Neurophysiology: Official Journal of the International Federation of Clinical Neurophysiology. 2011; 122: 1588–1594. https://doi.org/10.1016/j.clinph.2011.01.011.

[6] Cull-Candy S, Brickley S, Farrant M. NMDA receptor subunits: diversity, development and disease. Current Opinion in Neurobiology. 2001; 11: 327–335. https://doi.org/10.1016/s0959-4388(00)00215-4.

[7] Kus L, Saxon D, Beitz AJ. NMDA R1 mRNA distribution in motor and thalamic-projecting sensory neurons in the rat spinal cord and brain stem. Neuroscience Letters. 1995; 196: 201–204. https://doi.org/10.1016/0304-3940(95)11878-z.

[8] Kalb RG, Lidow MS, Halsted MJ, Hockfield S. N-methyl-D-aspartate receptors are transiently expressed in the developing spinal cord ventral horn. Proceedings of the National Academy of Sciences of the United States of America. 1992; 89: 8502–8506. https://doi.org/10.1073/pnas.89.18.8502.

[9] Rivera C, Voipio J, Kaila K. Two developmental switches in GABAergic signalling: the K+-Cl- cotransporter KCC2 and carbonic anhydrase CAVII. The Journal of Physiology. 2005; 562: 27–36. https://doi.org/10.1113/jphysiol.2004.077495.

[10] Watanabe M, Wake H, Moorhouse AJ, Nabekura J. Clustering of neuronal K+-Cl- cotransporters in lipid rafts by tyrosine phosphorylation. The Journal of Biological Chemistry. 2009; 284: 27980–27988. https://doi.org/10.1074/jbc.M109.043620.

[11] Lee HHC, Deeb TZ, Walker JA, Davies PA, Moss SJ. NMDA receptor activity downregulates KCC2 resulting in depolarizing GABAA receptor-mediated currents. Nature Neuroscience. 2011; 14: 736–743. https://doi.org/10.1038/nn.2806.

[12] Zhou HY, Chen SR, Byun HS, Chen H, Li L, Han HD, *et al*. N-methyl-D-aspartate receptor- and calpain-mediated proteolytic cleavage of K+-Cl- cotransporter-2 impairs spinal chloride homeostasis in neuropathic pain. The Journal of Biological Chemistry. 2012; 287: 33853–33864. https://doi.org/10.1074/jbc.M112.395830.

[13] Creamer M, Cloud G, Kossmehl P, Yochelson M, Francisco GE, Ward AB, *et al*. Intrathecal baclofen therapy versus conventional medical management for severe poststroke spasticity: results from a multicentre, randomised, controlled, open-label trial (SISTERS). Journal of Neurology, Neurosurgery, and Psychiatry. 2018; 89: 642–650. https://doi.org/10.1136/jnnp-2017-317021.

[14] Chavez LM, Huang SS, MacDonald I, Lin JG, Lee YC, Chen YH. Mechanisms of Acupuncture Therapy in Ischemic Stroke Rehabilitation: A Literature Review of Basic Studies. International Journal of Molecular Sciences. 2017; 18: 2270. https://doi.org/10.3390/ijms18112270.

[15] Wang HQ, Hou M, Bao CL, Min L, Li H. Effects of Acupuncture Treatment on Lower Limb Spasticity in Patients Following

Hemorrhagic Stroke: A Pilot Study. European Neurology. 2019; 81: 5–12. https://doi.org/10.1159/000499133.

[16] Cai Y, Zhang CS, Zhang AL, Da Costa C, Xue CC, Wen Z. Electroacupuncture for Poststroke Spasticity: Results of a Pilot Pragmatic Randomized Controlled Trial. Journal of Pain and Symptom Management. 2021; 61: 305–314. https://doi.org/10.1016/j.jpainsymman.2020.07.034.

[17] Hu Y, Tang X, Li S, Liu P, Zhang K, Zhao L, *et al*. Electroacupuncture Improves the Motor Function in Rats with Spinal Cord Injury by Regulating UCN2-Mediated cAMP-PKA Signaling in the Spinal Cord Microenvironment. Cellular and Molecular Neurobiology. 2025; 45: 28. https://doi.org/10.1007/s10571-025-01537-1.

[18] Mu JD, Ma LX, Zhang Z, Yu WY, Sun TY, Qian X, *et al*. Acupuncture alleviates spinal hyperreflexia and motor dysfunction in post-ischemic stroke rats with spastic hypertonia via KCC2-mediated spinal $GABA_A$ activation. Experimental Neurology. 2022; 354: 114027. https://doi.org/10.1016/j.expneurol.2022.114027.

[19] McBride DW, Zhang JH. Precision Stroke Animal Models: the Permanent MCAO Model Should Be the Primary Model, Not Transient MCAO. Translational Stroke Research. 2017; 8: 397–404. https://doi.org/10.1007/s12975-017-0554-2.

[20] Longa EZ, Weinstein PR, Carlson S, Cummins R. Reversible middle cerebral artery occlusion without craniectomy in rats. Stroke. 1989; 20: 84–91. https://doi.org/10.1161/01.str.20.1.84.

[21] Chen J, Sanberg PR, Li Y, Wang L, Lu M, Willing AE, *et al*. Intravenous administration of human umbilical cord blood reduces behavioral deficits after stroke in rats. Stroke. 2001; 32: 2682–2688. https://doi.org/10.1161/hs1101.098367.

[22] Bohannon RW, Smith MB. Interrater reliability of a modified Ashworth scale of muscle spasticity. Physical Therapy. 1987; 67: 206–207. https://doi.org/10.1093/ptj/67.2.206.

[23] Chen CL, Chen CY, Chen HC, Wu CY, Lin KC, Hsieh YW, *et al*. Responsiveness and minimal clinically important difference of Modified Ashworth Scale in patients with stroke. European Journal of Physical and Rehabilitation Medicine. 2019; 55: 754–760. https://doi.org/10.23736/S1973-9087.19.05545-X.

[24] de Medinaceli L, Freed WJ, Wyatt RJ. An index of the functional condition of rat sciatic nerve based on measurements made from walking tracks. Experimental Neurology. 1982; 77: 634–643. https://doi.org/10.1016/0014-4886(82)90234-5.

[25] Beverungen H, Klaszky SC, Klaszky M, Côté MP. Rehabilitation Decreases Spasticity by Restoring Chloride Homeostasis through the Brain-Derived Neurotrophic Factor-KCC2 Pathway after Spinal Cord Injury. Journal of Neurotrauma. 2020; 37: 846–859. https://doi.org/10.1089/neu.2019.6526.

[26] Boulenguez P, Liabeuf S, Bos R, Bras H, Jean-Xavier C, Brocard C, *et al*. Down-regulation of the potassium-chloride cotransporter KCC2 contributes to spasticity after spinal cord injury. Nature Medicine. 2010; 16: 302–307. https://doi.org/10.1038/nm.2107.

[27] Bilchak JN, Yeakle K, Caron G, Malloy D, Côté MP. Enhancing KCC2 activity decreases hyperreflexia and spasticity after chronic spinal cord injury. Experimental Neurology. 2021; 338: 113605. https://doi.org/10.1016/j.expneurol.2021.113605.

[28] Thompson FJ, Reier PJ, Lucas CC, Parmer R. Altered patterns of reflex excitability subsequent to contusion injury of the rat spinal cord. Journal of Neurophysiology. 1992; 68: 1473–1486. https://doi.org/10.1152/jn.1992.68.5.1473.

[29] Monyer H, Sprengel R, Schoepfer R, Herb A, Higuchi M, Lomeli H, *et al*. Heteromeric NMDA receptors: molecular and functional distinction of subtypes. Science (New York, N.Y.). 1992; 256: 1217–1221. https://doi.org/10.1126/science.256.5060.1217.

[30] Bordelon JR, Smith Y, Nairn AC, Colbran RJ, Greengard P, Muly EC. Differential localization of protein phosphatase-1alpha, beta and gamma1 isoforms in primate prefrontal cortex. Cerebral Cortex (New York, N.Y.: 1991). 2005; 15: 1928–1937. https://doi.org/10.1093/cercor/bhi070.

[31] Wang Y, Lei Y, Fang L, Mu Y, Wu J, Zhang X. Roles of phosphatase 2A in nociceptive signal processing. Molecular Pain. 2013; 9: 46. https://doi.org/10.1186/1744-8069-9-46.

[32] Miazek A, Zalas M, Skrzymowska J, Bogin BA, Grzymajło K, Goszczynski TM, *et al*. Age-dependent ataxia and neurodegeneration caused by an αII spectrin mutation with impaired regulation of its calpain sensitivity. Scientific Reports. 2021; 11: 7312. https://doi.org/10.1038/s41598-021-86470-1.

[33] Chamma I, Heubl M, Chevy Q, Renner M, Moutkine I, Eugène E, *et al*. Activity-dependent regulation of the K/Cl transporter KCC2 membrane diffusion, clustering, and function in hippocampal neurons. The Journal of Neuroscience: the Official Journal of the Society for Neuroscience. 2013; 33: 15488–15503. https://doi.org/10.1523/JNEUROSCI.5889-12.2013.

[34] Zeng H, Chen J, Guo Y, Tan S. Prevalence and Risk Factors for Spasticity After Stroke: A Systematic Review and Meta-Analysis. Frontiers in Neurology. 2021; 11: 616097. https://doi.org/10.3389/fneur.2020.616097.

[35] Li S, Chen YT, Francisco GE, Zhou P, Rymer WZ. A Unifying Pathophysiological Account for Post-stroke Spasticity and Disordered Motor Control. Frontiers in Neurology. 2019; 10: 468. https://doi.org/10.3389/fneur.2019.00468.

[36] Sun TY, Ma LX, Mu JD, Zhang Z, Yu WY, Qian X, *et al*. Acupuncture improves the structure of spastic muscle and decreases spasticity by enhancing GABA, KCC2, and GABAAγ2 in the brainstem in rats after ischemic stroke. Neuroreport. 2022; 33: 399–407. https://doi.org/10.1097/WNR.0000000000001798.

[37] Li S, Francisco GE, Rymer WZ. A New Definition of Post-stroke Spasticity and the Interference of Spasticity With Motor Recovery From Acute to Chronic Stages. Neurorehabilitation and Neural Repair. 2021; 35: 601–610. https://doi.org/10.1177/15459683211011214.

[38] Niyo G, Almofeez LI, Erwin A, Valero-Cuevas FJ. A computational study of how an α- to γ-motoneurone collateral can mitigate velocity-dependent stretch reflexes during voluntary movement. Proceedings of the National Academy of Sciences of the United States of America. 2024; 121: e2321659121. https://doi.org/10.1073/pnas.2321659121.

[39] Lee S, Toda T, Kiyama H, Yamashita T. Weakened rate-dependent depression of Hoffmann's reflex and increased motoneuron hyperactivity after motor cortical infarction in mice. Cell Death & Disease. 2014; 5: e1007. https://doi.org/10.1038/cddis.2013.544.

[40] Ramírez-Jarquín UN, Tapia R. Excitatory and Inhibitory Neuronal Circuits in the Spinal Cord and Their Role in the Control of Motor Neuron Function and Degeneration. ACS Chemical Neuroscience. 2018; 9: 211–216. https://doi.org/10.1021/acschemneuro.7b00503.

[41] Zhu S, Noviello CM, Teng J, Walsh RM, Jr, Kim JJ, Hibbs RE. Structure of a human synaptic $GABA_A$ receptor. Nature. 2018; 559: 67–72. https://doi.org/10.1038/s41586-018-0255-3.

[42] Smith RJ, Cordeiro MH, Davey NE, Vallardi G, Ciliberto A, Gross F, *et al*. PP1 and PP2A Use Opposite Phospho-dependencies to Control Distinct Processes at the Kinetochore. Cell Reports. 2019; 28: 2206–2219.e8. https://doi.org/10.1016/j.celrep.2019.07.067.

[43] Shi GX, Yang CY, Wu MM, Guan LP, Wang LP, Liu CZ. Muscle hypertonia after permanent focal cerebral ischemia in rats: a qualitative and quantitative behavioral and electrophysiological study. The International Journal of Neuroscience. 2013; 123: 575–581. https://doi.org/10.3109/00207454.2013.783578.

[44] Côté MP, Murray LM, Knikou M. Spinal Control of Locomotion: Individual Neurons, Their Circuits and Functions. Frontiers in Physiology. 2018; 9: 784. https://doi.org/10.3389/fphys.2018.00784.

[45] Liu S, Wang Z, Su Y, Qi L, Yang W, Fu M, *et al*. A neuroanatomical basis for electroacupuncture to drive the vagal-adrenal axis. Nature. 2021; 598: 641–645. https://doi.org/10.1038/s41586-021-04001-4.

[46] Yang NN, Yang JW, Ye Y, Huang J, Wang L, Wang Y, *et al*. Electroacupuncture ameliorates intestinal inflammation by activating α7nAChR-mediated JAK2/STAT3 signaling pathway in postoperative ileus. Theranostics. 2021; 11: 4078–4089. https://doi.org/10.7150/thno.52574.